

# Lawrence Berkeley National Laboratory

## LBL Publications

### Title

Comparing the 2,2'-Biphenylenedithiophosphate Binding of Americium with Neodymium and Europium

### Permalink

<https://escholarship.org/uc/item/3zq898qx>

### Journal

Angewandte Chemie International Edition, 55(41)

### ISSN

1433-7851

### Authors

Cross, Justin N  
Macor, Joseph A  
Bertke, Jeffery A  
et al.

### Publication Date

2016-10-04

### DOI

10.1002/anie.201606367

### Supplemental Material

<https://escholarship.org/uc/item/3zq898qx#supplemental>

### Copyright Information

This work is made available under the terms of a Creative Commons Attribution-NonCommercial-NoDerivatives License, available at <https://creativecommons.org/licenses/by-nc-nd/4.0/>

Peer reviewed

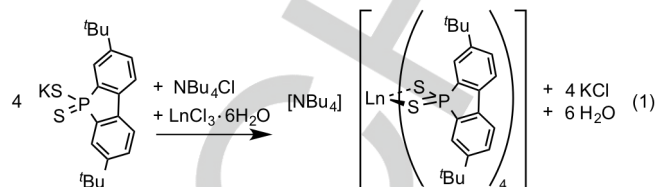
# Comparisons of Americium, Neodymium, and Europium Complexed by 2,2'-Biphenylenedithiophosphinate.

Justin N. Cross,<sup>1</sup> Joseph A. Macor,<sup>1,2</sup> Jeffery A. Bertke,<sup>2</sup> Maryline G. Ferrier,<sup>1</sup> Gregory S. Girolami,<sup>2\*</sup> Stosh A. Kozimor,<sup>1\*</sup> Joel R. Maassen,<sup>1</sup> Brian L. Scott,<sup>1</sup> David K. Shuh,<sup>4</sup> Benjamin W. Stein,<sup>1</sup> S. Chantal E. Stieber.<sup>1,3</sup>

**Abstract:** Advancing understanding of minor actinide (Am, Cm) versus lanthanide coordination chemistry is key for developing advanced nuclear fuel cycles. Owing to difficulties in accessing and handling Am and Cm, few reactivity and spectroscopic comparisons with lanthanides have been performed. Herein, we described the preparation of  $(\text{NBu}_4)\text{Am}[\text{S}_2\text{P}(\text{tBu}_2\text{C}_{12}\text{H}_6)_4]$  and two isomorphous lanthanide complexes, namely those with similar ionic radii (i.e.,  $\text{Nd}^{\text{III}}$ ) and that were isoelectronic ( $\text{Eu}^{\text{III}}$ ). The results included the first measurement of an Am–S bond length, mean 2.921(9) Å, by single crystal X-ray diffraction. Structural and spectroscopic comparisons with the  $\text{Eu}^{\text{III}}$  and  $\text{Nd}^{\text{III}}$  complexes revealed subtle electronic differences between  $\text{Am}^{\text{III}}$  and the lanthanides.

The implementation of advanced nuclear fuel cycles is critically dependent on developing effective methods to process spent fuel. One challenge associated with advancing nuclear fuel reprocessing is associated with separating minor actinides (Am and Cm) from their 4f-analogues. Owing to difficulties associated with conducting macroscopic experiments with Am and Cm, most insight into minor actinide/lanthanide separation chemistry comes from microchemical studies, where analyte quantities are more conveniently determined using  $\alpha$ ,  $\beta$ , and  $\gamma$ -spectroscopy.<sup>[1]</sup> This leaves many macroscopic chemical concepts poorly understood as there are limited structurally characterized trivalent pairs.<sup>[2]</sup>

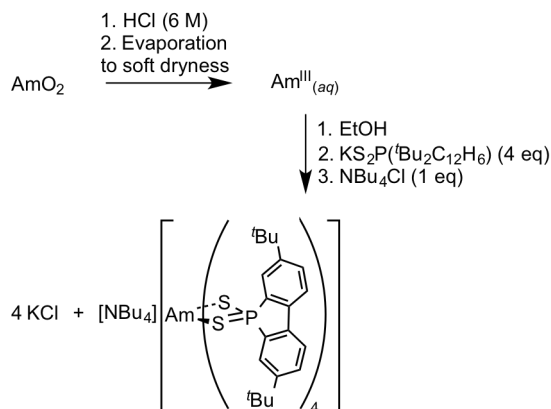
Of the many separation strategies that have a high probability for success,<sup>[3]</sup> those that employ dithiophosphate based extractants are of particular interest. To advance understanding of these dithiophosphate separations processes, we recently reported the syntheses of the 4,4'-di-*tert*-butyl-2,2'-biphenylenedithiophosphinic acid,  $\text{HS}_2\text{P}(\text{tBu}_2\text{C}_{12}\text{H}_6)$ , whose aryl ring orientations were constrained through C–C linkages.<sup>[4]</sup> We anticipated – based on previous studies – that constraining the rotameric orientation of the aryl rings provided a mechanism to control electronic factors that influenced selective binding to 5f over 4f elements.<sup>[5]</sup> Moreover, as the  $\text{HS}_2\text{P}(\text{tBu}_2\text{C}_{12}\text{H}_6)$  compound was air- and moisture-stable and soluble in a variety of common solvents, it provided an excellent opportunity to compare and contrast minor actinide and lanthanide coordination chemistry with identical dithiophosphate ligands. As such, this document compares dithiophosphate coordination chemistry of  $\text{Am}^{\text{III}}$  (5f<sup>6</sup>) with its electronic congener  $\text{Eu}^{\text{III}}$  (4f<sup>6</sup>) and its size-matched 4f-analogue,  $\text{Nd}^{\text{III}}$  (ionic radii = 1.109 and 1.108 Å).<sup>[2k,6,7]</sup> The isolation of the tetrakis(4,4'-di-



**Equation 1.**

*tert*-butyl-2,2'-biphenylenedithiophosphinato)metal(III) anions,  $\text{M}[\text{S}_2\text{P}(\text{tBu}_2\text{C}_{12}\text{H}_6)_4]^{-1}$  ( $\text{M} = \text{Am}, \text{Nd}, \text{Eu}$ ), enabled the first single-crystal measurement of an Am–S bond distance. Moreover, the structural results – alongside the UV-vis and fluorescence data – provocatively, suggested that the  $\text{Am}^{\text{III}}\text{--S}_2\text{PR}_2$  interaction was electronically distinct from  $\text{Ln}\text{--S}_2\text{PR}_2$  bonds within analogous coordination environments.

Lanthanide complexes of the general formula  $(\text{NBu}_4)\text{Ln}[\text{S}_2\text{P}(\text{tBu}_2\text{C}_{12}\text{H}_6)_4]$  ( $\text{Ln} = \text{Nd}, \text{Eu}$ ) were prepared by salt metathesis reactions of potassium 4,4'-di-*tert*-butyl-2,2'-biphenylenedithiophosphinate,  $\text{KS}_2\text{P}(\text{tBu}_2\text{C}_{12}\text{H}_6)_4$ , with hydrated europium and neodymium trichlorides, followed by addition of tetrabutylammonium chloride,  $\text{NBu}_4\text{Cl}$ , Eq 1. As these synthetic procedures were quite robust, and routinely provided single crystals when carried out on either large (> 0.1 g) or small (< 0.01 g) scales, it seemed reasonable that similar methods would be successful in affording an americium analogue. The importance of scaling down these reactions cannot be overstated, as small-scale synthetic methods accounted for our limited inventory of <sup>243</sup>Am and the relatively high radioactivity associated with this isotope,  $t_{1/2} = 7370(40)$  y. As anticipated, the salt metathesis reaction generated the  $(\text{NBu}_4)\text{Am}[\text{S}_2\text{P}(\text{tBu}_2\text{C}_{12}\text{H}_6)_4]$  salt, Scheme 1. This procedure started by dissolving  $\text{AmO}_2$  in aqueous HCl (6 M), upon which  $\text{Am}^{\text{IV}}$  reduced to  $\text{Am}^{\text{III}}$ . The resulting  $\text{Am}^{\text{III}}$  solution was evaporated to a soft dryness, which left a peach colored residue. Subsequently, the residue was suspended in ethanol and treated with ethanolic solutions of  $\text{KS}_2\text{P}(\text{tBu}_2\text{C}_{12}\text{H}_6)_4$  and  $\text{NBu}_4\text{Cl}$ . For all three complexes, block-shaped single crystals were obtained from slow evaporation of ethanol solutions. Figure 1



**Scheme 1.** Synthesis of  $(\text{NBu}_4)\text{Am}[\text{S}_2\text{P}(\text{tBu}_2\text{C}_{12}\text{H}_6)_4]$ .

<sup>1</sup> Los Alamos National Laboratory, Los Alamos, New Mexico 87545

<sup>2</sup> University of Illinois at Urbana-Champaign, Urbana, Illinois 61801

<sup>3</sup> California State Polytechnic University, Pomona California 91768

<sup>4</sup> Lawrence Berkeley National Laboratory, Berkeley California 94720

ggirolami@illinois.edu, stosh@lanl.gov

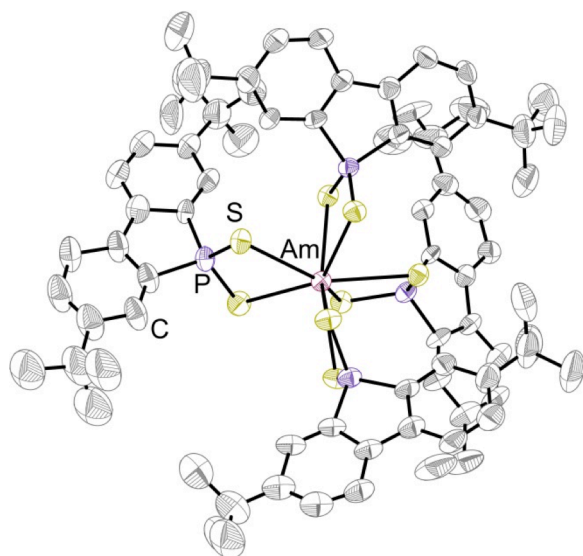


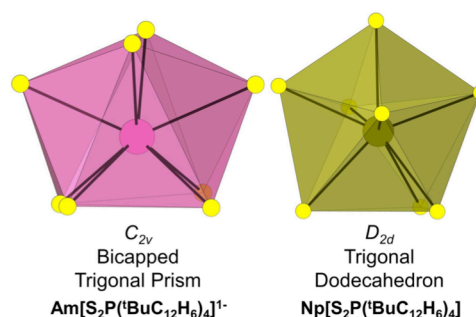
**Figure 1.** Thermal ellipsoid plot of  $(\text{NBu}_4)\text{Am}[\text{S}_2\text{P}(\text{Bu}_2\text{C}_{12}\text{H}_6)_4]_4^{1-}$ . Thermal ellipsoids are drawn with 30% probability.  $\text{NBu}_4^+$  counter-cation and hydrogen – atoms were omitted. Key: C (gray), P (purple), S (yellow), Am (pink).

shows a thermal ellipsoid plot of  $\text{Am}[\text{S}_2\text{P}(\text{Bu}_2\text{C}_{12}\text{H}_6)_4]_4^{1-}$ , while similar plots for  $\text{Ln}[\text{S}_2\text{P}(\text{Bu}_2\text{C}_{12}\text{H}_6)_4]_4^{1-}$  ( $\text{Ln} = \text{Nd}, \text{Eu}$ ) were provided in the SI. Structural metrics from the isomorphous  $(\text{NBu}_4)\text{M}[\text{S}_2\text{P}(\text{Bu}_2\text{C}_{12}\text{H}_6)_4]$  ( $\text{M} = \text{Am}, \text{Eu}, \text{Nd}$ ) complexes were compared in Table 1. Somewhat unexpectedly, the  $\text{M}^{\text{III}}[\text{S}_2\text{P}(\text{Bu}_2\text{C}_{12}\text{H}_6)_4]_4^{1-}$  ( $\text{M}^{\text{III}} = \text{Eu}, \text{Nd}, \text{Am}$ ) geometries were different than those reported previously for tetravalent  $\text{M}^{\text{IV}}[\text{S}_2\text{P}(\text{Bu}_2\text{C}_{12}\text{H}_6)_4]$  ( $\text{M}^{\text{IV}} = \text{U}, \text{Np}$ ) compounds, even though all of these species consisted of  $f$ -element ions coordinated by four  $\text{S}_2\text{P}(\text{Bu}_2\text{C}_{12}\text{H}_6)_4^{1-}$  ligands.<sup>[4]</sup> For instance, Raymond's *Shape8* routine showed the eight sulfur atoms in the inner sphere of  $\text{M}^{\text{III}}[\text{S}_2\text{P}(\text{Bu}_2\text{C}_{12}\text{H}_6)_4]_4^{1-}$  ( $\text{M} = \text{Eu}, \text{Nd}, \text{Am}$ ) formed a distorted bicapped trigonal prism with approximate  $C_{2v}$  symmetry, Scheme 2.<sup>[6]</sup> In contrast, the *Shape8* analysis indicated the +4 actinides in  $\text{M}^{\text{IV}}[\text{S}_2\text{P}(\text{Bu}_2\text{C}_{12}\text{H}_6)_4]$  ( $\text{M} = \text{U}, \text{Np}$ ) adopted a distorted trigonal dodecahedral geometry with approximate  $D_{2d}$  symmetry.

The  $\text{Am}[\text{S}_2\text{P}(\text{Bu}_2\text{C}_{12}\text{H}_6)_4]_4^{1-}$  structure enabled the Am–S bond length to be measured for the first time by single crystal X-ray diffraction. The Am–S bond distances varied by approximately 0.1 Å and ranged from 2.887(4) to 2.969(4) Å. These distances agreed well with previously reported EXAFS data from the  $\text{Am}^{\text{III}}$  complex extracted by bis(2,4,4-trimethylphenyl)dithiophosphinic acid,  $\text{HS}_2\text{P}[\text{C}_6\text{H}_5]_2$  (cyanex-301), into kerosene.<sup>[10]</sup> A plot of mean M–S distances in  $\text{M}[\text{S}_2\text{P}(\text{Bu}_2\text{C}_{12}\text{H}_6)_4]_4^{x-}$  complexes ( $\text{M} = \text{Eu}, \text{Nd}, \text{Am}$  and  $x = 1$ ;  $\text{M} =$

**Table 1.** Average bond lengths and angles (with calculated standard error)<sup>[9]</sup> in  $(\text{NBu}_4)\text{M}[\text{S}_2\text{P}(\text{Bu}_2\text{C}_{12}\text{H}_6)_4]$  ( $\text{M} = \text{Nd}, \text{Eu}, \text{Am}$ ).

Average Bond Lengths (Å)			
	Nd	Eu	Am
M–S	2.941(8)	2.910(9)	2.921(9)
M–P	3.525(8)	3.498(8)	3.52(1)
Average Bond Angles (°)			
	Nd	Eu	Am
S–M–S	68.6(5)	69.1(5)	68.3(3)
S–P–S	112.1(6)	111.4(6)	111.4(8)



**Scheme 2.** Comparison of the first coordination environments from  $\text{Am}[\text{S}_2\text{P}(\text{Bu}_2\text{C}_{12}\text{H}_6)_4]_4^{1-}$  and  $\text{Np}[\text{S}_2\text{P}(\text{Bu}_2\text{C}_{12}\text{H}_6)_4]_4^{1-}$ .

$\text{U}, \text{Np}$  and  $x = 0$ ) versus the metal ionic radii<sup>[2k, 6]</sup> (Figure 2) showed a linear relationship for the  $\text{Eu}^{\text{III}}, \text{Nd}^{\text{III}}, \text{U}^{\text{IV}},$  and  $\text{Np}^{\text{IV}}$  structures. The data was fit with a line whose slope approached unity, 0.89(2), and whose y-intercept [1.95(2) Å] was approximately equal to the  $\text{S}^{2-}$  ionic radius, 1.84 Å.<sup>[6]</sup> Interestingly, the observed average Am–S distances of 2.921(9) Å (uncertainty determined as the error of the mean)<sup>[9]</sup> in  $\text{Am}[\text{S}_2\text{P}(\text{Bu}_2\text{C}_{12}\text{H}_6)_4]_4^{1-}$  was 0.02 Å shorter than expected from this linear relationship. While tempting to attribute the slightly shorter Am–S distance to increased Am–S covalency, we refrained as the structural deviations were only marginally relevant statistically. Instead, these results serve as motivation for future S K-edge XAS measurements, to determine quantitatively the degree of S 3p- and Am 5f-/6d-mixing.

The absorption spectra from  $\text{M}^{\text{III}}[\text{S}_2\text{P}(\text{Bu}_2\text{C}_{12}\text{H}_6)_4]_4^{1-}$  ( $\text{M} = \text{Eu}, \text{Nd}, \text{Am}$ ) were collected from single crystals using a microspectrophotometer (Figure 3). All spectra showed an intense peak at high energies, likely associated with charge transfer transitions. For  $\text{Nd}^{\text{III}}$  and  $\text{Am}^{\text{III}}$ , weak Laporte forbidden  $f \rightarrow f$  transitions were also present.<sup>[11]</sup> As observed previously for  $(\text{NEt}_4)\text{Eu}[\text{S}_2\text{P}(\text{C}_6\text{H}_5)_2]_4$ ,<sup>[12]</sup> analogous transitions for  $\text{Eu}[\text{S}_2\text{P}(\text{Bu}_2\text{C}_{12}\text{H}_6)_4]_4^{1-}$  were engulfed in the charge transfer band.

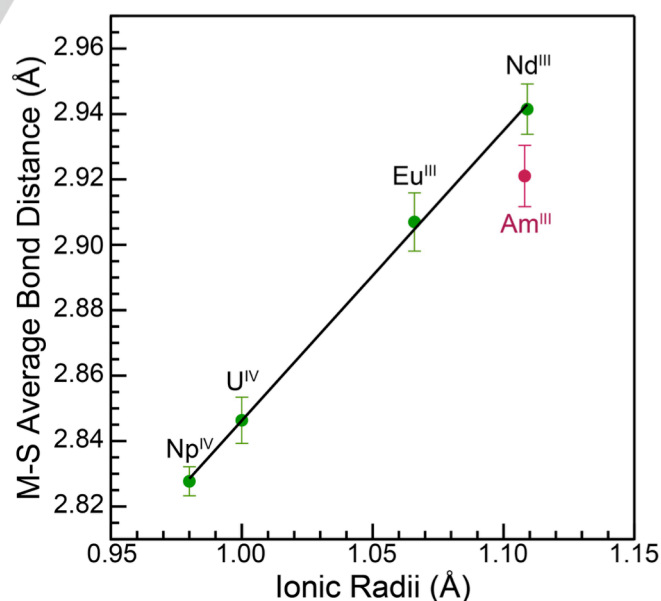


**Figure 2.** A plot showing the relationship between the M–S Average Bond distances from  $(\text{NBu}_4)\text{M}^{\text{III}}[\text{S}_2\text{P}(\text{Bu}_2\text{C}_{12}\text{H}_6)_4]_4^{1-}$  ( $\text{M} = \text{Eu}, \text{Nd}, \text{Am}$ ) and  $\text{M}^{\text{IV}}[\text{S}_2\text{P}(\text{Bu}_2\text{C}_{12}\text{H}_6)_4]$  ( $\text{M} = \text{U}, \text{Np}$ )<sup>[4]</sup> versus the metal ionic radii.<sup>[6]</sup>

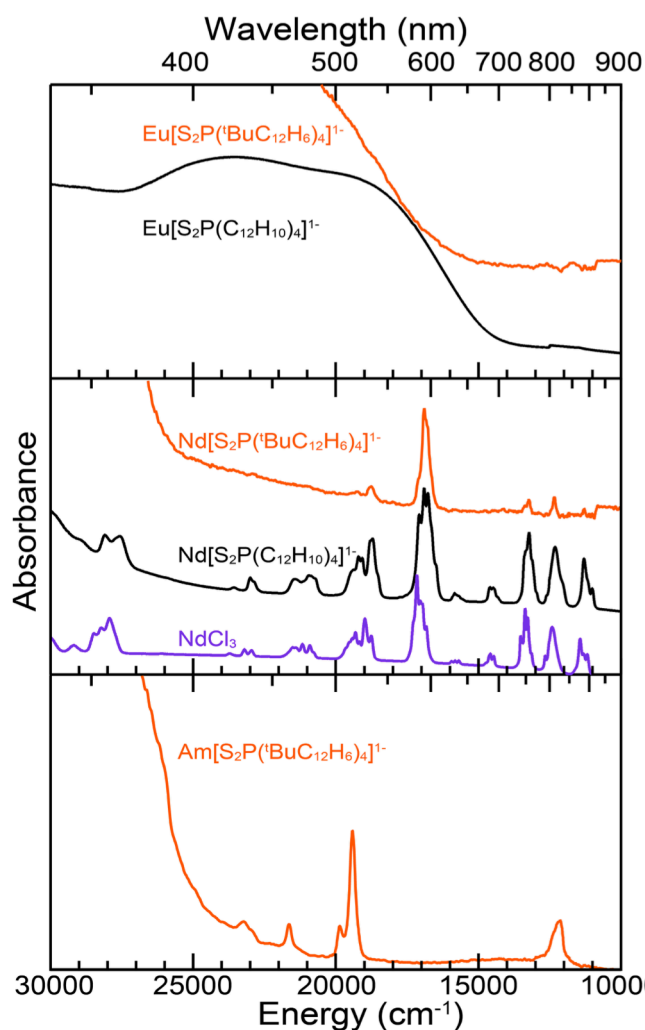


**Figure 3.** UV-vis-NIR absorption spectra of single crystals of  $(\text{NBu}_4)\text{M}[\text{S}_2\text{P}(\text{Bu}_2\text{C}_{12}\text{H}_6)_4]$  ( $\text{M} = \text{Eu}, \text{Nd}, \text{Am}$ ; orange traces),  $[\text{Z}][\text{Ln}[\text{S}_2\text{P}(\text{C}_6\text{H}_5)_2]_4]$  ( $\text{Ln} = \text{Eu}, \text{Z} = \text{PPH}_4$ ;  $\text{Nd}, \text{Z} = \text{NEt}_4$ ; black traces), and  $\text{NdCl}_3$  (purple trace). Spectra obtained from single crystals of  $\text{M}[\text{S}_2\text{P}(\text{Bu}_2\text{C}_{12}\text{H}_6)_4]^{-1}$  were obtained in transmission mode whereas  $\text{Ln}[\text{S}_2\text{P}(\text{C}_6\text{H}_5)_2]_4^{-1}$  and  $\text{LnCl}_3$  data were acquired from powders by diffuse reflectance.

Figure 3 additionally compared data from  $\text{Nd}[\text{S}_2\text{P}(\text{Bu}_2\text{C}_{12}\text{H}_6)_4]^{-1}$  with absorption spectra obtained from  $(\text{NEt}_4)\text{Nd}[\text{S}_2\text{P}(\text{C}_6\text{H}_5)_2]_4$  and  $\text{NdCl}_3$ .<sup>[12]</sup> These three spectra were similar and showed characteristic  $\text{Nd}^{\text{III}} 4f \rightarrow 4f$  transitions. Peak assignments were determined based on previous spectral interpretations and described from the perspective of the free ion.<sup>[11]</sup> For example, we attributed the visible transitions to excitations from the  $\text{Nd}^{\text{III}} 4f_{9/2}$  ground state to  $4G_{7/2}$ ,  $4G_{5/2}$ , and  $2H_{9/2}$  excited states. Although, a slight bathochromic shift ( $\sim 1$  to  $10$  nm) was observed upon moving from  $\text{NdCl}_3$  to  $\text{Nd}[\text{S}_2\text{P}(\text{C}_6\text{H}_5)_2]_4^{-1}$ , the spectral regions containing  $4f \rightarrow 4f$  transitions from  $\text{Nd}[\text{S}_2\text{P}(\text{C}_6\text{H}_5)_2]_4^{-1}$  and  $\text{Nd}[\text{S}_2\text{P}(\text{Bu}_2\text{C}_{12}\text{H}_6)_4]^{-1}$  were nearly superimposable. The similar energies for the  $4f \rightarrow 4f$  transitions suggested that ligand field contributions for  $\text{Nd}[\text{S}_2\text{P}(\text{Bu}_2\text{C}_{12}\text{H}_6)_4]^{-1}$ ,  $\text{Nd}[\text{S}_2\text{P}(\text{C}_6\text{H}_5)_2]_4^{-1}$ , and  $\text{NdCl}_3$  were small.

The absorption spectrum from  $\text{Am}[\text{S}_2\text{P}(\text{Bu}_2\text{C}_{12}\text{H}_6)_4]^{-1}$  contained weak and narrow peaks at 428, 435, 461, 503, 514,

and 818 nm that could be assigned to  $5f \rightarrow 5f$  transitions (Figure 3). In accord with previous interpretations of  $\text{Am}^{\text{III}}$  optical spectra,<sup>[13]</sup> the spectrum from  $\text{Am}[\text{S}_2\text{P}(\text{Bu}_2\text{C}_{12}\text{H}_6)_4]^{-1}$  involved excitations from the  $\text{Am}^{\text{III}} 7F_0'$  ground state to the  $5H_4'$ ,  $2G_2'$ ,  $5D_2'$ ,  $5L_6'$ ,  $7F_6'$ , and  $7F_4'$  excited states, respectively. While this interpretation was also described in terms of the free ion, all the  $\text{Am}^{\text{III}}$  term symbols included a prime mark ('') that served as a reminder to treat the actinides in the so-called intermediate and spin angular momentum eigenvalues  $L$  and  $S$  are no longer "good" quantum numbers owing to the effect of  $j-j$  coupling.<sup>[13]</sup> The  $\text{Am}[\text{S}_2\text{P}(\text{Bu}_2\text{C}_{12}\text{H}_6)_4]^{-1} 5f \rightarrow 5f$  peak energies and line shapes substantially differed ( $>100$  nm) from reports on other americium compounds, such as  $\text{Am}(\text{C}_5\text{H}_5)_3$ ,<sup>[13b]</sup>  $\text{AmX}_3$  ( $\text{X} = \text{Cl}, \text{Br}, \text{I}$ ),<sup>[13a]</sup>  $\text{Am}_2(\text{HPO}_3)_3(\text{H}_2\text{O})$ ,<sup>[2k]</sup> and  $\text{Am}[\text{B}_9\text{O}_{13}(\text{OH})_4] \cdot \text{H}_2\text{O}$ .<sup>[2g]</sup> Overall, these results suggested that the ligand field exerts a greater influence on the electronic structure of  $\text{Am}^{\text{III}}$  than it does on  $4f$  ions, the latter exhibiting spectra that are essentially invariant from compound to compound (see above).

The luminescence spectra obtained from single crystals of  $(\text{AsPh}_4)\text{S}_2\text{P}(\text{Bu}_2\text{C}_{12}\text{H}_6)$  (prepared previously<sup>[4])</sup>  $\text{Eu}[\text{S}_2\text{P}(\text{Bu}_2\text{C}_{12}\text{H}_6)_4]^{-1}$ ,  $\text{Nd}[\text{S}_2\text{P}(\text{Bu}_2\text{C}_{12}\text{H}_6)_4]^{-1}$ , and  $\text{Am}[\text{S}_2\text{P}(\text{Bu}_2\text{C}_{12}\text{H}_6)_4]^{-1}$  were provided in Figure 4. The  $\text{S}_2\text{P}(\text{Bu}_2\text{C}_{12}\text{H}_6)^{-1}$  free ligand luminesced when excited at 365 and 420 nm. This ligand-based fluorescence persisted upon complexation with  $f$ -elements, and appeared alongside characteristic metal-based emission lines. For example,  $\text{Eu}[\text{S}_2\text{P}(\text{Bu}_2\text{C}_{12}\text{H}_6)_4]^{-1}$  showed strong red emission with emission peaks centered at 590, 612, 651, and 700 nm, which were typical of  $\text{Eu}^{\text{III}}$ . From the free ion perspective, these features can be described as arising from relaxations of the  $5D_0$  state to the  $7F_1$ ,  $7F_2$ ,  $7F_3$ , and  $7F_4$  states respectively.<sup>[14]</sup>

Metal-based luminescence from  $\text{Nd}[\text{S}_2\text{P}(\text{Bu}_2\text{C}_{12}\text{H}_6)_4]^{-1}$  and  $\text{Am}[\text{S}_2\text{P}(\text{Bu}_2\text{C}_{12}\text{H}_6)_4]^{-1}$  were less intense than that from the europium analogue. In both cases excitation at 365 and 420 nm generated weak and broad luminescence peaks in the visible region and sharp emission peaks in the near-infrared. For  $\text{Nd}[\text{S}_2\text{P}(\text{Bu}_2\text{C}_{12}\text{H}_6)_4]^{-1}$ , relaxation of the  $4F_{3/2}$  excited state to the  $4I_{9/2}$  ground state was observed as an emission near 880 nm.<sup>[15]</sup> Unfortunately, limitations associated with our single crystal spectrometer inhibited obtaining the complete spectrum, and the emission peak was only partially observed. The  $\text{Am}[\text{S}_2\text{P}(\text{Bu}_2\text{C}_{12}\text{H}_6)_4]^{-1}$  emission spectrum provided a rarely observed phenomenon of americium-based luminescence. The spectrum contained a clear emission peak at 700 nm and a weaker peak at 855 nm. The assignments of these peaks were based on interpretations of the limited number of other americium emission spectra.<sup>[20,16]</sup> These features were attributed to relaxations from the  $5D_1'$  excited state to the  $7F_1'$  and  $7F_2'$  ground states, respectively. Additionally, a small feature near 600 nm was also associated with americium-based emission, specifically the  $5D_1' \rightarrow 7F_0'$  transition.

Given the difficulty in acquiring the relatively long-lived  $^{243}\text{Am}$  isotope ( $t_{1/2} = 7370(40)$  y, care was taken in recycling the  $^{243}\text{Am}$  sample for future studies. This procedure was carried out using slight variations of published radioanalytical methods.<sup>[17]</sup> Our process involved digesting  $\text{Am}[\text{S}_2\text{P}(\text{Bu}_2\text{C}_{12}\text{H}_6)_4]^{-1}$  with aqua regia in a sealed autoclave at 200 °C and subsequent purification using cation exchange chromatography. Samples

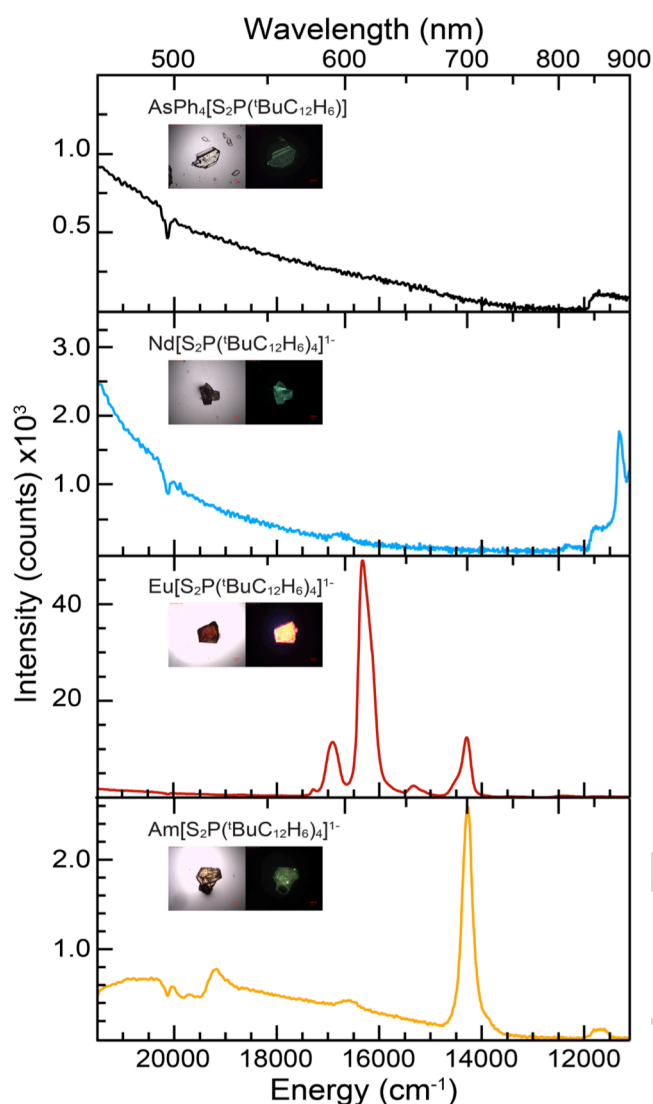


**Figure 4.** UV-vis-NIR luminescence spectra of single crystals of  $(\text{AsPh}_4)[\text{S}_2\text{P}(\text{Bu}_2\text{C}_{12}\text{H}_6)_4]$  (black), and  $(\text{NBu}_4)\text{M}[\text{S}_2\text{P}(\text{Bu}_2\text{C}_{12}\text{H}_6)_4]$ , ( $\text{M} = \text{Eu}$  red,  $\text{Nd}$  blue,  $\text{Am}$  green). Visible colors in  $\text{AsPh}_4$ ,  $\text{Nd}$ , and  $\text{Am}$  salts arise from ligand based emission.

were loaded onto the column in dilute acid (5 drops conc.  $\text{HCl}$  in 5 mL  $\text{H}_2\text{O}$ ) and, washed with  $\text{HCl}$  (0.1 M). The column effluent was analyzed using  $\gamma$ -spectroscopy and ICP-AES, which showed that the majority of the S, P, and  $^{239}\text{Np}$  ( $^{243}\text{Am}$  daughter nuclide) were not retained (Figure 5). After chemical purification, increasing the chloride content of the mobile phase ( $\text{HCl}$  conc) led to  $\text{Am}^{\text{III}}$  elution. Analysis of the  $\text{Am}^{\text{III}}$  fractions showed high  $\text{Am}^{\text{III}}$  recovery (>99 %) and that the dithiophosphinate byproducts were completely removed (Further details in the SI).

The well-defined coordination complexes described herein afforded a rarely available opportunity to explore how the chemical and physical properties vary as a function of  $5f$ - versus  $4f$ -metal identity ( $\text{Am}^{\text{III}}$ ,  $\text{Nd}^{\text{III}}$  and  $\text{Eu}^{\text{III}}$ ). These comparisons revealed structural and electronic differences between isomorphous complexes that contained isoelectronic metals ( $\text{Eu}$ ,  $4f^6$ ;  $\text{Am}$ ,  $5f^6$ ) and  $5f$ - and  $4f$ -metals of nearly identical radii ( $\text{Am}^{\text{III}}$  and  $\text{Nd}^{\text{III}}$ ). Additionally, the study enabled the first single crystal X-ray diffraction measurement of an  $\text{Am-S}$  bond. The structural, optical absorption, and luminescent studies subtly suggested

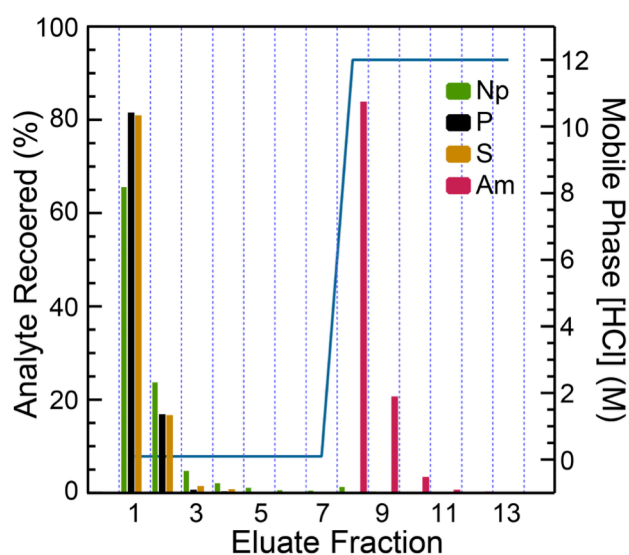


**Figure 5.** Representative elution profile of the americium recovery process using AG50W-X8 (100 to 200 mesh). Analyte recovery (%; left-axis) and the concentration of  $\text{HCl}$  (M; right-axis; blue trace) in the mobile phase was plotted against the eluate fraction number. The  $^{239}\text{Np}$  (green) and  $^{243}\text{Am}$  (red) amounts were quantified using  $\gamma$ -spectroscopy, while S (yellow) and P (black) were measured by ICP-AES. Fraction 1 represents the load, fractions 2 – 7 washes ( $\text{HCl}$  0.1 M); and 8 – 13  $^{243}\text{Am}$  elution ( $\text{HCl}$  12 M).

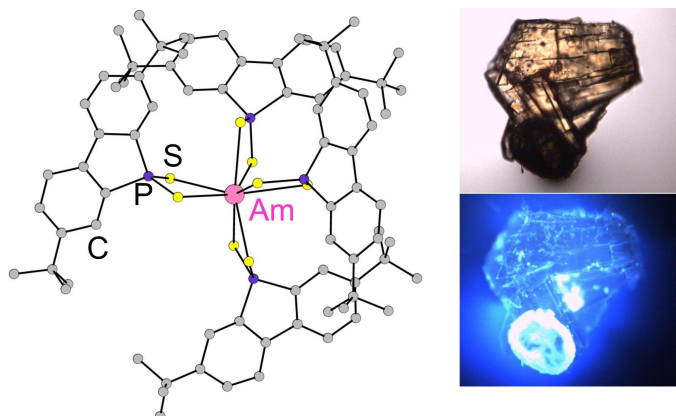
that the biphenylenedithiophosphinate ligand field influenced the  $\text{Am}^{\text{III}}$  electronic structure to a greater extent than in analogous lanthanide systems. These  $f$ -element dithiophosphinate complexes constitute an excellent test bed for theoretical and spectroscopic studies to advance understanding of  $f$ -element electronic structure and bonding. It is our hope that the anticipated advances in  $f$ -element electronic structure will further fundamental understanding in support of developing advanced nuclear fuel cycles.

## Acknowledgements

We are grateful to the United States Department of Energy, Office of Science, Isotope Development and Production for Research and Application subprogram within Office of Nuclear Physics for support and for supplying the  $^{243}\text{Am}$  isotope used in these studies. Research efforts were supported under the Heavy Element Chemistry Program at LANL by the Division of Chemical Sciences, Geosciences, and Biosciences, Office of Basic Energy Sciences, U.S. Department of Energy (Kozimor, Scott). Los Alamos National Laboratory is operated by Los Alamos National Security, LLC, for the National Nuclear Security Administration of U.S. Department of Energy (contract DE-AC52-06NA25396). Efforts at LBNL (Shuh) were supported by the Director, Office of Science, Office of Basic Energy Sciences, Division of Chemical Sciences, Geosciences, and Biosciences Heavy Element Chemistry Program of the U.S. Department of Energy at Lawrence Berkeley National Laboratory under Contract No. DE-AC02-05CH11231. We additionally thank the Office of Nuclear Energy Fuel Cycle R&D Program (Macor). Portions of this work were also supported by postdoctoral and graduate Fellowships from the Glenn T. Seaborg Institute (Macor, Ferrier, Stein, Stieber), and the Director's Postdoctoral Fellowship (Cross). Work at the University of Illinois was funded in part by the National Science Foundation under grant CHE 13-62931 to Girolami.

**Keywords:** Radiochemistry • X-ray diffraction • Americium • Electronic Absorption • Actinide • Inorganic Chemistry

- [1] a) R. M. Diamond, K. Street, G. T. Seaborg, *J. Am. Chem. Soc.* **1954**, *76*, 1461. b) H. L. Smith, D. C. Hoffman, *J. Inorg. Nucl. Chem.* **1956**, *3*, 243. c) G. R. Choppin, *J. Less-Common Met.* **1983**, *93*, 323. d) K. L. Nash, R. E. Barrans, R. Chiarizia, M. L. Dietz, M. P. Jensen, P. G. Rickert, B. A. Moyer, P. V. Bonnesen, J. C. Bryan, R. A. Sachleben, *Solvent Extr. Ion. Exc.* **2000**, *18*, 605. e) M. P. Jensen, A. H. Bond, *J. Am. Chem. Soc.*, **2002**, *124*, 9870. f) M. Miguiditchian, D. Guillauneux, D. Guillaumont, P. Moisy, C. Madic, M. P. Jensen, K. L. Nash, *Inorg. Chem.* **2005**, *44*, 1404. g) D. Girnt, P. W. Roesky, A. Geist, C. M. Ruff, P. J. Panak, M. A. Denecke, *Inorg. Chem.*, **2010**, *49*, 9627.
- [2] a) J. H. Burns, J. R. Peterson, *Acta Crystallogr. Sect. B* **1970**, *26*, 1885; b) J. H. Burns, J. R. Peterson, J. N. Stevenson, *J. Inorg. Nucl. Chem.* **1975**, *37*, 743; c) J. H. Matonic, B. L. Scott, M. P. Neu, *Inorg. Chem.* **2001**, *40*, 2638; d) P. Lindqvist-Reis, C. Apostolidis, J. Rebizant, A. Morgenstern, R. Klenze, O. Walter, T. Fanghaenel, R. G. Haire, *Angew. Chem. Int. Ed.* **2007**, *46*, 919; e) C. Apostolidis, B. Schimmelpfennig, N. Magnani, P. Lindqvist-Reis, O. Walter, R. Sykora, A. Morgenstern, E. Colineau, R. Caciuffo, R. Klenze, R. G. Haire, J. Rebizant, F. Bruchertseifer, T. Fanghanel, *Angew. Chem. Int. Ed.* **2010**, *49*, 6343; f) A. E. Enriquez, J. H. Matonic, B. L. Scott, M. P. Neu, *Chem. Commun.* **2003**, 1892; g) M. J. Polinski, S. Wang, E. V. Alekseev, W. Depmeier, T. E. Albrecht-Schmitt, *Angew. Chem. Int. Ed.* **2011**, *50*, 8891; h) M. J. Polinski, D. J. Grant, S. Wang, E. V. Alekseev, J. N. Cross, E. M. Villa, W. Depmeier, L. Gagliardi, T. E. Albrecht-Schmitt, *J. Am. Chem. Soc.* **2012**, *124*, 10682; i) M. J. Polinski, S. Wang, J. N. Cross, E. V. Alekseev, W. Depmeier, T. E. Albrecht-Schmitt, *Inorg. Chem.* **2012**, *51*, 7859; j) M. J. Polinski, S. Wang, E. V. Alekseev, W. Depmeier, G. Liu, R. G. Haire, T. E. Albrecht-Schmitt, *Angew. Chem. Int. Ed.* **2012**, *51*, 1869; k) J. N. Cross, E. M. Villa, S. Wang, J. Diwu, M. J. Polinski, T. E. Albrecht-Schmitt, *Inorg. Chem.* **2012**, *51*, 8419; l) M. J. Polinski, K. A. Pace, J. Stritzinger, J. Lin, J. N. Cross, S. K. Cary, S. M. V. Cleve, E. V. Alekseev, T. E. Albrecht-Schmitt, *Chem. Eur. J.* **2014**, *20*, 9892; m) W. Runde, A. C. Bean, L. F. Brodnax, B. L. Scott, *Inorg. Chem.* **2006**, *45*, 2479; n) R. E. Sykora, Z. Assefa, R. G. Haire, T. E. Albrecht-Schmitt, *J. Solid State Chem.* **2005**, *177*, 4413; o) R. E. Sykora, Z. Assefa, R. G. Haire, T. E. Albrecht-Schmitt, *Inorg. Chem.* **2005**, *44*, 5667; p) C. Tamain, B. Arab-Chapelet, M. Rivenet, X. F. Legoff, G. Loubert, S. Grandjean, F. Abraham, *Inorg. Chem.* **2015**, *55*, 51; q) S. K. Cary, M. Vasiliu, R. E. Baumbach, J. T. Stritzinger, T. D. Green, K. Diefenbach, J. N. Cross, K. L. Knappenberger, G. Liu, M. A. Silver, A. E. DePrince, M. J. Polinski, S. M. V. Cleve, J. H. House, N. Kikugawa, A. Gallagher, A. A. Arico, D. A. Dixon, T. E. Albrecht-Schmitt, *Nat. Comm.* **2015**, *6*, 6827.
- [3] a) Z. Kolarik, *Chem. Rev.*, **2008**, *108*, 4208. b) P. J. Panak, A. Geist, *Chem. Rev.*, **2013**, *113*, 1199. c) M. J. Hudson, L. M. Harwood, D. M. Laventine, F. W. Lewis, *Inorg. Chem.*, **2013**, *52*, 3414. d) Y. Zhu, J. Chen, R. Jiao, *Solvent Extr. Ion Exch.*, **1996**, *14*, 61. e) C. Madic, M. J. Hudson, J.-O. Liljenzin, J.-P. Glatz, R. Nannicini, A. Facchini, Z. Kolarik, R. Odoj, *Prog. Nucl. Energy*, **2002**, *40*, 523. f) B. Weaver, F. A. Kappelmann, *J. Inorg. Nucl. Chem.*, **1968**, *30*, 263. g) M. Nilsson, K. L. Nash, *Solvent Extr. Ion Exch.*, **2007**, *25*, 665. h)
- [4] J. A. Macor, J. L. Brown, J. N. Cross, S. R. Daly, A. J. Gaunt, G. S. Girolami, M. T. Janicke, S. A. Kozimor, M. P. Neu, A. C. Olson, S. D. Reilly, B. L. Scott, *Dalton Trans.* **2015**, *44*, 18923.
- [5] S. R. Daly, J. M. Keith, E. R. Batista, K. S. Boland, D. L. Clark, S. A. Kozimor, R. L. Martín, *J. Am. Chem. Soc.* **2012**, *134*, 14408.
- [6] Shannon, R. D. *Acta Crystallogr.* **1976**, *A55*, 5135.
- [7] F. H. David, *J. Less-Common Met.* **1986**, *121*, 29.
- [8] a) A. E. Gorden, J. Xu, K. N. Raymond, *Chem. Rev.* **2003**, *103*, 4207; b) J. Xu, E. Radkov, M. Ziegler, K. N. Raymond, *Inorg. Chem.* **2000**, *39*, 4156.
- [9] D. C. Harris in *Quantitative Chemical Analysis*, 8 Ed., W. H. Freeman and Company, New York, **2010**, pp. 62-64.
- [10] G. Tian, Y. Zhu, J. Xu, T. Hu, Y. Xie, *J. Alloys Compd.* **2002**, *334*, 86.
- [11] K. Binnemans, C. Goerler-Walrand, *Chem. Phys. Lett.* **1995**, *235*, 163.
- [12] K. S. Boland, D. E. Hobart, S. A. Kozimor, M. M. MacInnes, B. L. Scott, *Polyhedron* **2014**, *67*, 540.
- [13] a) R. G. Pappalardo, W. T. Carnall, P. R. Fields, *J. Chem. Phys.* **1969**, *51*, 1182; b) R. Pappalardo, W. T. Carnall, P. R. Fields, *J. Chem. Phys.* **1969**, *51*, 842.
- [14] a) K. Binnemans, *Coord. Chem. Rev.* **2015**, *295*, 1; b) P. A. Tanner, *Chem. Soc. Rev.* **2013**, *42*, 5090.
- [15] a) S. Yanagida, Y. Hasegawa, K. Murakoshi, Y. Wada, N. Nakashima, T. Yamanaka, **1998**, *171*, 461; b) R. Janicki, A. Mondry, *Eur. J. Inorg. Chem.* **2013**, *19*, 3429.
- [16] a) A. B. Yusov, *J. Radioanal. Nucl. Chem.* **1990**, *143*, 287; b) Z. Assefa, K. Kalachnikova, R. G. Haire, R. E. Sykora, *J. Solid State Chem.* **2007**, *180*, 3121; c) W. H. Runde, W. W. Shulz in *The Chemistry of Actinide and Transactinide Elements* (Eds.: L. R. Morss, N. M. Edelstein, J. Fuger), Springer Netherlands, Dordrecht, **2011**, pp. 1265; d) M. Sturzbecher-Hoehne, P. Yang, A. D'Aleo, R. J. Abergel, *Dalton Trans.* **2016**, *45*, 9912.
- [17] a) R. A. Penneman, T. K. Keenan in *The Radiochemistry of Americium and Curium*, Technical Information Center U.S. Atomic Energy Commission, Washington D.C. **1960**, pp 15; b) J. Kleinberg, *LA-1721 5<sup>th</sup> Ed. Collected Radiochemical and Geochemical Procedures*, Los Alamos National Lab, Los Alamos, **1990**, pp 203.



$\text{Am}[\text{S}_2\text{P}(\text{tBu}_2\text{C}_{12}\text{H}_9)]_4$ ; Am–S mean = 2.921(9) Å

The synthesis and spectroscopy of an americium biphenylenedithiophosphinate complex is described. The first single crystal measurement of an Am–S bond was achieved with a mean distance of 2.921(9) Å. The complex also features  $\text{Am}^{\text{III}}$  luminescence. The above photograph shows a crystal under white light and excitation at 365 nm.